Molecular Cancer Therapeutics

Transient Exposure to Quizartinib Mediates Sustained Inhibition of FLT3 Signaling while Specifically Inducing Apoptosis in FLT3-Activated Leukemia Cells

Ruwanthi N. Gunawardane, Ronald R. Nepomuceno, Allison M. Rooks, Jeremy P. Hunt, Jill M. Ricono, Barbara Belli, and Robert C. Armstrong

Abstract

Fms-like tyrosine kinase 3 (FLT3) is implicated in the pathogenesis of acute myeloid leukemia (AML). FLT3-activating internal tandem duplication (ITD) mutations are found in approximately 30% of patients with AML and are associated with poor outcome in this patient population. Quizartinib (AC220) has previously been shown to be a potent and selective FLT3 inhibitor. In the current study, we expand on previous observations by showing that quizartinib potently inhibits the phosphorylation of FLT3 and downstream signaling molecules independent of FLT3 genotype, yet induces loss of viability only in cells expressing constitutively activated FLT3. We further show that transient exposure to quizartinib, whether *in vitro* or *in vivo*, leads to prolonged inhibition of FLT3 signaling, induction of apoptosis, and drastic reductions in tumor volume and pharmacodynamic endpoints. *In vitro* experiments suggest that these prolonged effects are mediated by slow binding kinetics that provide for durable inhibition of the kinase following drug removal/clearance. Together these data suggest quizartinib, with its unique combination of selectivity and potent/sustained inhibition of FLT3, may provide a safe and effective treatment against FLT3-driven leukemia. *Mol Cancer Ther; 12(4); 438–47. ©2013 AACR.*

Introduction

Fms-like tyrosine kinase 3 (FLT3) is a member of the type III receptor tyrosine kinase (RTK) family and is required during early hematopoiesis (1). Deregulation of FLT3 is often found in the blast cells of leukemias including acute myeloid leukemia (AML) and acute lymphoblastic leukemia (ALL; refs. 2, 3). Approximately 30% of patients with AMLs harbor gain-of-function FLT3 internal tandem duplication (ITD) mutations that drive constitutive activation of downstream signaling cascades and are associated with poor disease outcome (4–7). Beyond activating mutations, overexpression of FLT3 and/or coexpression of the endogenous FLT3 ligand (FL) represent additional mechanisms by which FLT3 may be pathogenically activated (8). Activation of FLT3 kinase results in FLT3 autophosphorylation and induction of multiple downstream signaling cascades including the Ras/MAPK, PI3K/Akt, and STAT5 pathways (1, 9–13). In general, cells that have activated FLT3 are thought to be "addicted" to FLT3 signaling for their survival and growth, thereby rendering them exquisitely sensitive to FLT3-targeted therapy (14).

Multiple small-molecule FLT3 inhibitors, including lestaurtinib, sunitinib, sorafenib, tandutinib, and midostaurin, have been evaluated clinically (2, 15–22). Although these inhibitors were shown to be efficacious against FLT3-activated cell lines *in vitro* and in preclinical efficacy models (19, 23–28), clinical results to date have been disappointing due to dose-limiting toxicity and lack of durable responses in patients with AMLs (22, 29). With the exception of tandutinib, these inhibitors are multi-kinase inhibitors that lack FLT3, or even RTK, selectivity (30). The undesirable off-target effects of these compounds may have prevented administration of sufficiently high doses to achieve complete and sustained FLT3 inhibition. Nevertheless, the few responses observed in patients with AMLs with these inhibitors were often accompanied by inhibition of constitutive FLT3 phosphorylation (15, 25, 31, 32), suggesting that more potent, selective, and durable inhibition of FLT3 may result in a broader and more significant response in patients with AMLs.

Quizartinib/AC220, is a small-molecule kinase inhibitor that potently inhibits FLT3 with a high degree of kinome selectivity (30). We have previously shown the

Authors' Affiliation: Ambit Biosciences, San Diego, California

Note: Supplementary data for this article are available at Molecular Cancer Therapeutics Online (http://mct.aacrjournals.org/).

Current address for R.N. Gunawardane: Amgen Inc., 1201 Amgen Court West, Seattle, WA 98119; and Current address for J.P. Hunt: DiscoveRx, 11180 Roselle Street, Suite D, San Diego, CA 92121.

Corresponding Author: Robert C. Armstrong, Ambit Biosciences, Corp, 11080 Roselle St., San Diego, CA 92121. Phone: 858-334-2104; Fax: 858-334-2192; E-mail: barmstrong@ambitbio.com

doi: 10.1158/1535-7163.MCT-12-0305

potent inhibition by quizartinib of cellular FLT3 autophosphorylation and cell viability in the FLT3-ITD cell line, MV4-11, and the translation of this potent inhibition into effective antitumor activity in tumor xenograft models (30). A recent phase I clinical study of quizartinib in patients with AMLs indicates that continuous, once-daily administration of this drug can lead to reduced FLT3 signaling and tumor burden, as more than 50% of FLT3-ITD patients and a smaller percentage of patients without the ITD mutation, had a partial or complete response to treatment (unpublished data).

To better understand the mechanism of FLT3-mediated efficacy of quizartinib, we evaluated its inhibitory activity across different FLT3 isoforms, its impact on downstream FLT3 signaling pathways and the durability of this inhibition *in vitro* and *in vivo*. These studies reveal quizartinib to be a potent inhibitor of FLT3 signaling across a variety of FLT3 genotypes yet triggers apoptosis only in cells with endogenously activated FLT3. Furthermore, we show that slow quizartinib dissociation from FLT3 may cause sustained inhibition of FLT3 autophosphorylation and downstream signaling, induction of cell death *in vitro*, and achievement of a durable response in human tumor xenografts following a single administration. These results suggest that quizartinib may be unique among clinical FLT3 inhibitors with respect to potency, specificity, and durability of FLT3 inhibition.

Materials and Methods

Reagents

Quizartinib (FLT3; K_d = 1.6 nmol/L), lestaurtinib (FLT3; K_d = 8.5 nmol/L), midostaurin (FLT3; K_d = 11 nmol/L), and sorafenib (FLT3; K_d = 13 nmol/L) were synthesized at Ambit Biosciences (30). Tandutinib (FLT3; K_d = 3 nmol/L), was custom-synthesized by CiVenti-Chem, and sunitinib (FLT3; K_d = 0.5 nmol/L) was custom-synthesized by Sai Advantium, Ltd. (all K_d values from ref. 30). Antibodies for immunoblot analysis were purchased as follows: FLT3, extracellular signal–regulated kinase (Erk1/2), phospho-Erk1/2 (T202/Y204), and β-actin from Santa Cruz Biotechnology, Inc.; Akt, phospho-Akt (S473), PARP, cleaved PARP (D214), and phospho-STAT5 (Y694) from Cell Signaling Technology; STAT5 from BD Biosciences; and phosphotyrosine (pTyr; 4G10) from Millipore. Culture media were obtained from MediaTech and FBS from Omega Scientific. Except where noted, all other reagents were obtained from Sigma-Aldrich.

Cell culture

MV4-11, RS4;11, THP-1, and HEL 92.1.7 (HEL) cells were obtained from American Type Culture Collection (ATCC). Cell lines were authenticated at ATCC before purchase by their standard short tandem repeat DNA typing methodology. MOLM-14 and SEM-K2 cells were a gift from Dr. Mark Levis (Johns Hopkins Medical School, Baltimore, MD). Within 1 month of receipt, cultures were grown out for several passages and aliquots of each were frozen. For experimental use, each cell type was thawed and grown out for no more than 2 months before use in an experiment. The cells were maintained in 10% FBS in IMDM (MV4-11), RPMI-1640 (MOLM-14 and SEM-K2), and RPMI-1640 supplemented with D-glucose, HEPES, 2 mmol/L L-glutamine, sodium bicarbonate, and sodium pyruvate (HEL, RS4;11, and THP-1). Cells were serum-starved overnight in medium containing 0.5% FBS before treatment with compound for immunoblots and viability assays.

Immunoprecipitation of FLT3

Serum-starved cells were washed with cold PBS. RS4;11 cells were either untreated or treated for 15 minutes with 100 ng/mL human FL (R&D Systems) before the PBS wash. For quizartinib treatment, serum-starved MV4-11 cells were incubated with a dose titration of quizartinib for 2 hours. Twenty million MV4-11 cells were used for each dose. Cells were washed with cold PBS and lysed for 20 minutes on ice with Cell Extraction Buffer (Invitrogen) supplemented with protease (Roche Applied Science) and phosphatase (EMD Chemicals) inhibitor cocktails and 1 mmol/L phenylmethylsufonyl fluoride (PMSF). Following a 15-minute centrifugation to clear the lysate, 2 mg of lysate was incubated with FLT3 antibody for 16 hours at 4°C. Protein A-agarose was added to this mixture and incubated for 2 hours at 4°C. Bead complexes were washed 3 times with Cell Extraction Buffer and proteins eluted with NuPAGE LDS Sample Buffer (Invitrogen). FLT3 immunoprecipitates were analyzed by SDS-PAGE and immunoblotting for phospho-tyrosine and total-FLT3 content.

Immunoblot analysis

Immunoprecipitates or 50 μg of whole-cell lysates were separated by SDS-PAGE, transferred to nitrocellulose, and immunoblotted with primary antibodies overnight at 4°C. Fluorescent secondary antibodies (LI-COR Biosciences) used for detection were incubated for 30 minutes at room temperature. Blots were scanned using the LI-COR Odyssey Infrared Imaging System, and bands were quantified using this system's application software.

FLT3 and STAT5 immunoassays

Following overnight culture in low serum (0.5% FBS), cells were seeded at 400,000 cells per well in a 96-well plate and treated with inhibitors as described above. Following compound incubation, FLT3 phosphorylation was induced in RS4;11 and THP-1 cells with 100 ng/mL FL for 15 or 5 minutes, respectively. Cell lysates (Cell Lysis Buffer from Cell Signaling Technology supplemented with protease and phosphatase inhibitor cocktails and 1 mmol/L PMSF) were cleared by centrifugation. Phosphorylated and total STAT5a/b levels in the lysates were determined using the Multi-Spot Phospho-(Tyr 694); Total STAT5a/b assay from Meso Scale Discovery (MSD) as instructed by the manufacturer. Levels of phosphorylated and total FLT3 in the

lysates were similarly determined using the MSD electrochemiluminescence platform as previously described (30). All IC_{50} calculations were conducted using IGOR Pro 5 software (WaveMetrics) on data normalized to dimethyl sulfoxide (DMSO)-treated cells.

Cell viability assays

Serum-deprived cells were seeded at a density of 50,000 (MV4-11), 30,000 (MOLM-14), or 60,000 (SEM-K2, RS4;11, and THP-1) cells per well in a 96-well plate and then treated with DMSO or a dose titration of inhibitors. CellTiter-Blue (CTB) reagent (Promega) was added to the cells after 3 or 7 days following inhibitor addition. The resulting fluorescent signals were measured after 3 hours using a fluorescence plate reader. Viability was calculated as a percentage of cells treated with DMSO.

PARP cleavage assays

Cells starved overnight were incubated with a dose titration of quizartinib for 24 hours (MV4-11), 6 days (SEM-K2), or 7 days (RS4;11). Cells were lysed and subjected to immunoblot analysis as described above for cleaved and uncleaved PARP.

Durability experiments with washouts

For CTB viability assays, cells treated as described above were incubated with drug for 30 minutes, 24 hours, or 48 hours, washed 3 times with PBS, followed by addition of fresh low-serum media and incubated such that the total assay time was 72 hours for each. Control cells were treated with compounds continuously for 72 hours with no washout. Viability was measured using CTB as described above. For phosphorylated FLT3 and STAT5 analyses, serum-starved cells were treated with compound for 2 hours washed with PBS as above, replenished with fresh media containing 0.5% FBS, then further incubated for 30 minutes, 6 or 24 hours before cell lysis and MSD immunoassay analysis as described above. Control cells with no recovery time were lysed immediately following the 2-hour compound treatment. Structures for the inhibitors used in these experiments (quizartinib, lestaurtinib, and sorafenib) are found in Fig. 5.

Kinetic binding assays

Binding assays were conducted as described previously (33). The assays measure the ability of a test compound to compete with the interaction between a kinase and a known ATP site—binding ligand that has been immobilized on a solid support using quantitative PCR. Binding reactions were incubated for 90 minutes and either left undiluted or diluted as indicated. These reactions were measured at 20 and 120 minutes post-dilution.

In vivo efficacy model

Female C.B-17 SCID mice (Harlan Laboratories) were implanted subcutaneously on day 0 with 5×10^6 MV4-11 cells in a 50:25:25 homogeneous mixture of PBS and High/Low concentration Basement Membrane Matrigel (BD Biosciences). Treatments began when the mean estimated tumor mass for all groups (10 mice per group) reached about 250 mm^3. Quizartinib, formulated in 5% hydroxypropyl-β-cyclodextrin, was administered at 1 or 10 mg/kg by oral gavage once a day for 1 day or 14 consecutive days. Animals with tumors in excess of 2,000 mm^3 or with excessive ulcerated tumors were euthanized as were those found in obvious distress or in a moribund condition. Body weights and tumor measurements were recorded 3 times weekly. Tumor burden was estimated from caliper measurements by the formula for the volume of a prolate ellipsoid assuming unit density as: tumor burden (mm^3) = $(L \times W^2)/2$, where L and W are the respective orthogonal tumor length and width measurements in mm. Tumor growth inhibition (T/C, %) and tumor growth delay (T-C, days) were each calculated relative to the predefined endpoint of 1,500 mm^3 as previously defined (34).

Tumor lysates

When tumor volume reached approximately 300 mm^3, animals received a single dose of 1 or 10 mg/kg quizartinib by oral gavage. Tumors were harvested at various time points post-dose and were extracted with ice-cold Cell Extraction Buffer supplemented with protease and phosphatase inhibitor cocktails and 1 mmol/L PMSF using mechanical dissociation. Tumor extracts were analyzed for phosphorylated FLT3 by MSD immunoassay and for phosphorylated STAT5, AKT, ERK, and cleaved PARP levels by immunoblotting as described above.

Results

Quizartinib is a potent inhibitor of FLT3 autophosphorylation in wild-type and ITD-mutated FLT3 cells

To explore the impact of *FLT3* genotype on quizartinib-mediated FLT3 inhibition, we expanded on an earlier study (30) to include a panel of 5 leukemia cell lines expressing wild-type (WT) or ITD-mutated FLT3. MV4-11 cells are homozygous for the *FLT3-ITD* mutation, whereas MOLM-14 cells harbor both a WT and ITD allele (35). RS4;11, THP-1, and SEM-K2 cells are each homozygous for WT *FLT3*; however, SEM-K2 cells have an amplification of the *FLT3* gene leading to elevated expression and constitutive activation of FLT3 (Fig. 1A and B). MV4-11 and MOLM-14 cells also have constitutively activated FLT3 as a result of the ITD mutation, whereas RS4;11 and THP-1 cells require FL for activation/phosphorylation of the receptor (Fig. 1B and data not shown). Similar to its effects on MV4-11 cells (30), quizartinib potently downregulated the autophosphorylation of FLT3 in MOLM-14 and SEM-K2 cells and FL-stimulated FLT3 phosphorylation in RS4;11 and THP-1 cells (Table 1 and Supplementary Fig. S1). While slightly higher IC_{50} values were observed in the FLT3-WT cells compared with the FLT3-ITD cells (4- to 9-fold), these results indicate that quizartinib is a potent inhibitor of FLT3 phosphorylation irrespective of genotype and ranks among the most potent when compared with a panel of FLT3 inhibitors (Supplementary Table S1).

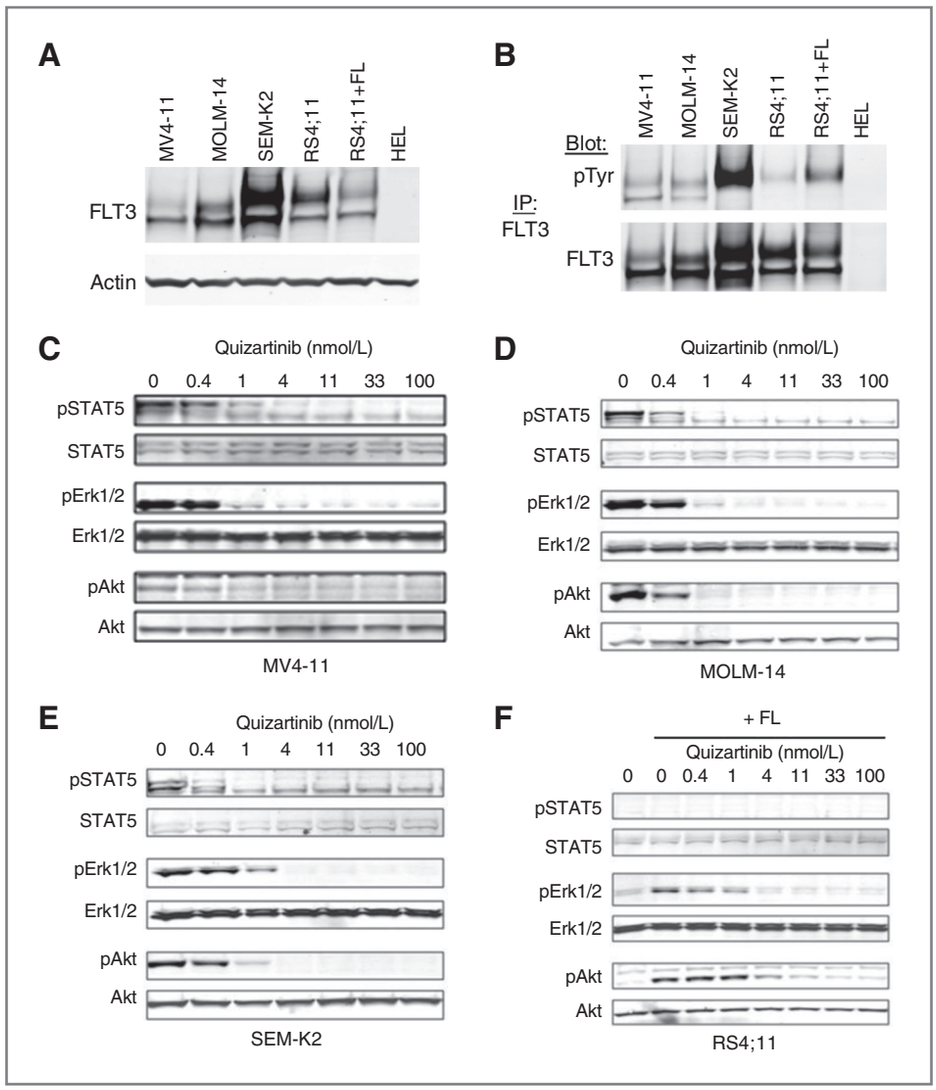

Figure 1. FLT3 expression profile in cell panel and quizartinib-mediated inhibition of STAT5, Erk, and Akt. A, expression levels of FLT3 receptor were tested by immunoblot analysis from untreated MV4-11, MOLM-14, and SEM-K2 and from RS4;11 cells treated for 15 minutes without or with 100 ng/mL FL (+FL). HEL cells were used for a negative control cell lysate. B, phospho-FLT3 in leukemia cell lines. FLT3 was immunoprecipitated from cells treated as in A and probed with anti-phosphotyrosine (pTyr; top) and anti-FLT3 (bottom) antibodies. C–F, MV4-11, MOLM-14, SEM-K2, and RS4;11 cells were treated with DMSO vehicle or the indicated amounts of quizartinib for 2 hours and the lysates were analyzed by immunoblot for total and phosphorylated STAT5, Erk1/2, and Akt. RS4;11 cells were stimulated with 100 ng/mL FL (+FL) for 15 minutes before cell lysis as indicated.

Inhibition of FLT3-mediated signaling pathways

Constitutive and ligand-induced activation of FLT3 leads to phosphorylation of downstream effector molecules in signaling networks such as the STAT5, Ras/MAPK, and PI3K/Akt pathways. Consistent with FLT3 inhibition, quizartinib potently inhibited phosphorylation of constitutively activated STAT5, Erk1/2, and Akt in MV4-11, MOLM-14, and SEM-K2 cells with IC_{50} values in the range of 0.3 to 0.7 nmol/L, and of FL-stimulated phosphorylation of Erk1/2 and Akt in RS4;11 cells with IC_{50} values of 0.3 and 3 nmol/L, respectively (Fig. 1C–F, Table 1 and Supplementary Fig. S1). Consistent with previous reports (12, 13, 36), STAT5 is not constitutively phosphorylated, nor does FL induce its phosphorylation in RS4;11 cells (Fig. 1F). Taken together, these results show that quizartinib-mediated FLT3 inhibition, in either FLT3-ITD or–WT cells, is accompanied by potent attenuation of downstream signaling events.

Quizartinib inhibits cell survival in FLT3-activated cells

To determine whether FLT3 genotype would influence the sensitivity of cells to FLT3 inhibition with respect to cell viability, we assessed cell viability across the cell panel following treatment with quizartinib. Both of the FLT3-ITD cell lines, MV4-11 and MOLM-14, were exquisitely sensitive to quizartinib treatment with cell viability IC_{50} values of 0.1 to 0.3 nmol/L measured at 72 hours (Fig. 2A, Table 1). Interestingly, while an IC_{50} of 0.4 nmol/L could be measured after 72 hours in SEM-K2 cells, complete loss of viability required 5 to 7 days (Fig. 2A and B, Table 1). In contrast, minimal or no loss of viability was observed in the FLT3-WT–expressing RS4;11 and THP-1 cells (Fig. 2A and B, Table 1), even following 7 days of quizartinib treatment, consistent with reports that these lines are not dependent on FLT3 signaling for sustained cell growth (18, 37). Importantly, comparison of quizartinib to a panel of FLT3 inhibitors revealed similar rank

Table 1. Signaling and cell viability profile for quizartinib

	IC_{50}, nmol/L				
Assay	**MV4-11**	**MOLM-14**	**SEM-K2**	**RS4;11**	**THP-1**
pFLT3	0.9	1.7	4	4.4	8.3
pSTAT5	0.7	0.2	0.3	ND	ND
pErk	0.5	0.4	0.7	0.3	ND
pAkt	0.6	0.3	0.7	3.1	ND
Viability	0.3	0.1	0.4	>10,000	>10,000

Abbreviation: ND, not determined.

order across the cell panel discussed above, with quizartinib showing the greatest FLT3 potency and selectivity toward FLT3-activated cells especially compared with some of the less FLT3-selective inhibitors (Supplementary Table S1).

Quizartinib induces apoptosis in FLT3-activated cells

Treatment with quizartinib induced significant and dose-dependent PARP cleavage and accumulation of sub-2N DNA in MV4-11, MOLM-14, and SEM-K2 cells (Fig. 2C and Supplementary Fig. S2). Cleavage was observed as

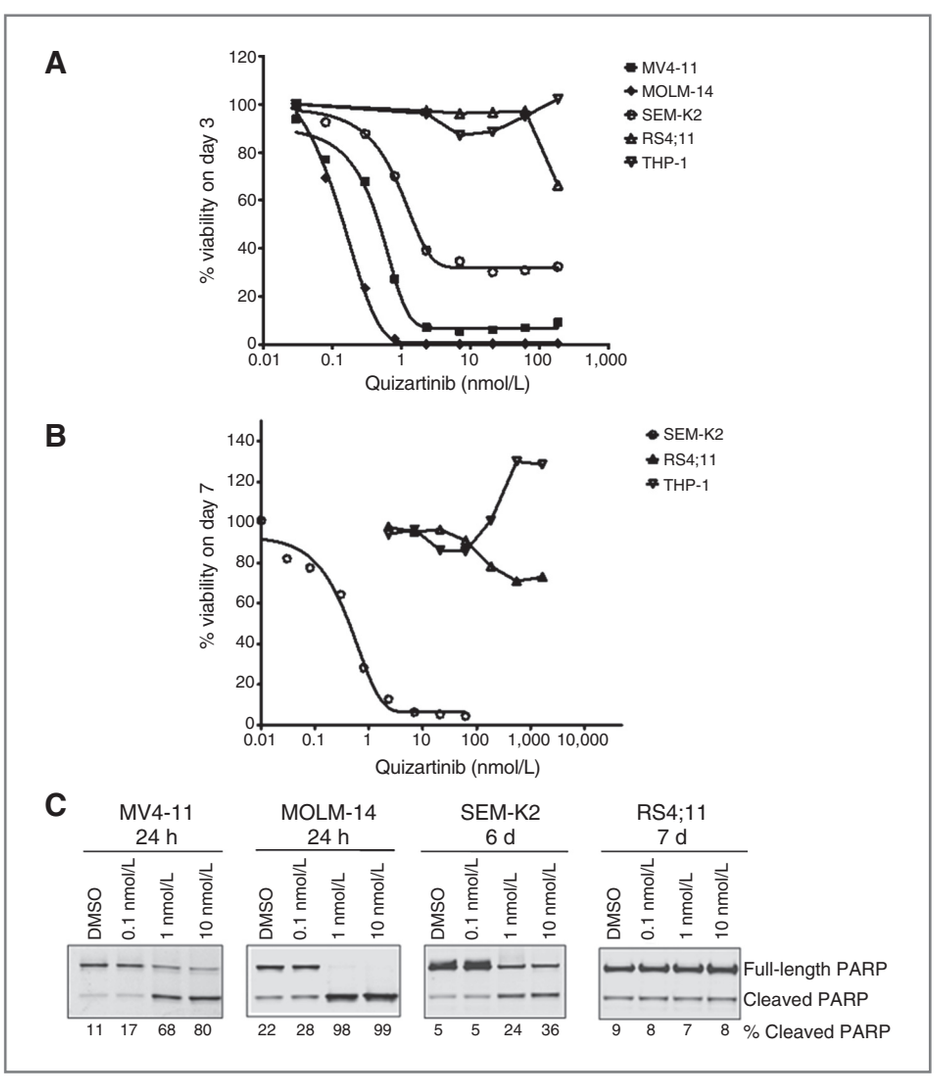

Figure 2. Differential sensitivity of leukemia cell viability and apoptosis upon quizartinib treatment. Cell viability was measured 3 (A) or 7 (B) days after compound addition. Percentage of viability was calculated on the basis of DMSO-treated control cells. C, immunoblot analysis of PARP cleavage in cells treated with DMSO or the indicated amounts of quizartinib for 24 hours (MV4-11 and MOLM-14), 6 days (SEM-K2), or 7 days (RS4;11). The percentage of cleaved PARP was calculated as the amount of cleaved PARP divided by the sum of cleaved PARP and full-length PARP.

Table 2. IC_{50} values for washout experiments in MV4-11

Washout duration	No wash	0.5 h	6 h	24 h
Compound incubation time				
pFLT3, IC_{50}, nmol/L				
Quizartinib	1.1	0.9	1.3	1.1
Lestaurtinib	2.0	5.6	8.2	15.9
Sorafen	1.0	1.0	2.3	2.7
pSTAT5, IC_{50}, nmol/L				
Quizartinib	0.3	0.4	0.7	0.7
Lestaurtinib	0.3	0.4	1.3	1.3
Sorafenib	0.5	0.4	1.1	1.6
	72 h	**48 h**	**24 h**	**0.5 h**
Compound exposure time				
Cell viability, IC_{50}, nmol/L				
Quizartinib	0.4	0.4	0.4	0.9
Lestaurtinib	1.9	5.9	12.5	60.8
Sorafenib	0.7	1.5	0.9	4.6

early as 8 (data not shown) and 24 hours after quizartinib treatment. Consistent with the effects of quizartinib on cell viability, significant PARP cleavage nor appearance of sub-2N DNA were observed in the SEM-K2 cells until 6 days posttreatment, whereas no increase in PARP cleavage or sub-2N DNA was observed in RS4;11 cells after 7 days of treatment (Fig. 2C and Supplementary Fig. S2).

Durability of quizartinib-mediated inhibition of FLT3 signaling

To assess the relative durability of quizartinib-mediated signaling inhibition in cell culture, we treated MV4-11 cells with quizartinib for 2 hours and then measured the levels of phosphorylated FLT3 (pFLT3) and STAT5 (pSTAT5) at 0.5, 6, and 24 hours after compound withdrawal (Table 2 and Supplementary Fig. S3). The approximately 1 nmol/L pFLT3 IC_{50} of quizartinib was maintained following a 0.5-, 6-, and even 24-hour washout period (Table 2). This durable inhibition translated to STAT5 phosphorylation as well, where no dramatic changes in IC_{50} values were observed under all 3 washout conditions tested (Table 2 and Supplementary Fig. S3). In contrast, lestaurtinib was found to be highly sensitive to the washouts resulting in about 3-, 4-, and 8-fold increase in pFLT3 IC_{50} following 0.5, 6, and 24 hours of drug removal (Table 2 and Supplementary Fig. S3). This translated to a 4-fold increase in the pSTAT5 IC_{50} values at the 6- and 24-hour washout. In parallel experiments, sorafenib showed a modest 2- to 3-fold increase in IC_{50} values for both pFLT3 and pSTAT5 (Table 2, Supplementary Fig. S3, and compound structures in Fig. 5).

Duration of compound exposure and loss of cell viability

To assess the impact of brief exposures on cell viability, MV4-11 cells were treated with compounds for various times, washed to remove inhibitors, and then assayed for viability 72 hours after initial exposure. Quizartinib exposures as short as 30 minutes led to virtually the same dose–response relationship as that achieved with continual 72 hours exposure (Table 2 and Supplementary Fig. S3). Under these conditions of brief quizartinib exposure, dose- and time-dependent increases in the pro-apoptotic Bim_{EL} were observed, along with decreases in the anti-apoptotic protein Mcl-1 (Supplementary Fig. S4). No changes in Bim_L Bim_S, Bax, Bcl-XL, or Bcl-2 were observed (Supplementary Fig. S4 and data not shown). Lestaurtinib was considerably more sensitive to compound removal with shorter exposures of lestaurtinib resulting in 3-, 7-, and 32-fold increases in IC_{50} for the 48-, 24-, and 0.5-hour exposures, respectively (Table 2 and Supplementary Fig. S3). Sorafenib-treated cells showed an intermediate sensitivity to compound removal (Table 2 and Supplementary Fig. 3). Similar durability properties were observed for each of these compounds in the MOLM-14 and SEM-K2 cells (data not shown). These results suggest that in cells dependent on constitutively activated FLT3, durable inhibition of FLT3 signaling following a brief exposure to quizartinib translates to lasting effects on cell viability mediated by modulation of pro- and anti-apoptotic proteins.

Time dependence of FLT3 binding

To understand how quizartinib mediates sustained FLT3 inhibition, we tested the effect of incubation time and dilution of the FLT3/inhibitor mixture on the apparent affinity of quizartinib to FLT3 using the kinase-binding technology described previously (33). To compare relative off-rates compounds were incubated with FLT3 for 1.5 hours followed by a series of dilutions and assayed for binding at 20 and 120 minutes. The binding curves generated from the diluted FLT3/quizartinib reactions were nearly identical to those of the undiluted reactions (Fig. 3A and B), as reflected in the 0.3 to 0.9 nmol/L K_d for all dilutions, and are indicative of a slow dissociation rate for quizartinib. In contrast, dilution of the FLT3/lestaurtinib binding reaction resulted in a clear shift in the binding curves corresponding to >30- and >100-fold increases in apparent K_d between no dilution and 50-fold dilution of the lestaurtinib/FLT3 mixture at each time point and is consistent with a rapid off-rate for lestaurtinib (Fig. 3C and D). Taken together, these binding data suggest that a slower quizartinib off-rate compared with lestaurtinib likely contributes to the differential effects these compounds show relative to FLT3 inhibition and cell viability described above.

In vivo efficacy and durability of FLT3 inhibition

To determine whether the durability properties of quizartinib *in vitro* translated to *in vivo* efficacy, we tested single-dose administrations of either 1 or 10 mg/kg quizartinib compared with the same doses given once per day for 14 days in the previously described MV4-11 xenograft model (30). Daily administration of 10 or

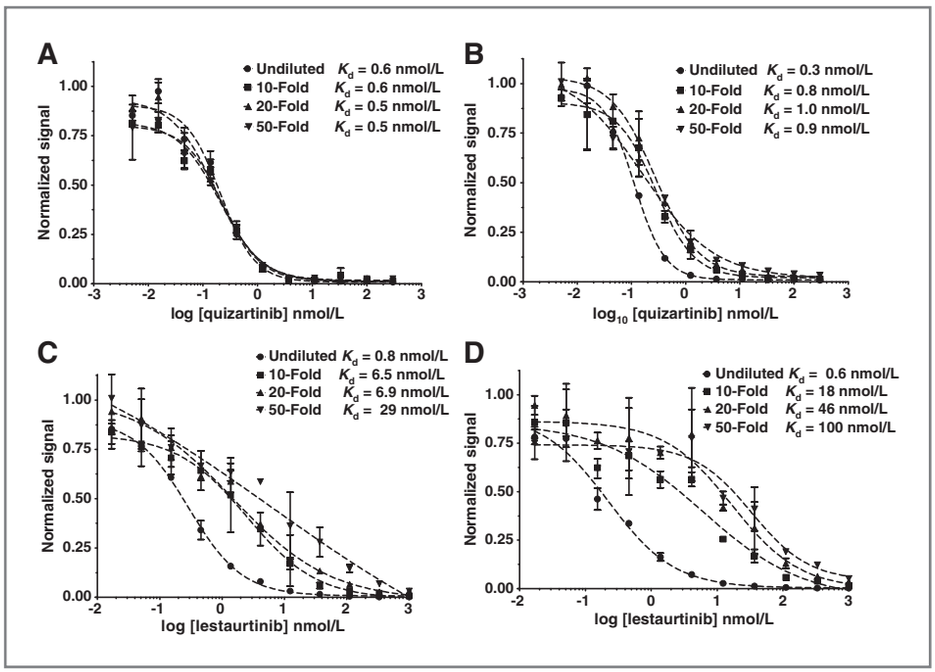

Figure 3. Time-dependent binding of quizartinib to FLT3. Quizartinib (A and B) and lestaurtinib (C and D) were preincubated with FLT3 for 1.5 hours and then diluted as indicated. The binding was measured either 20 minutes (A and C) or 2 hours (B and D) after dilution.

1 mg/kg quizartinib for 14 days led to significant tumor reduction consistent with our previous observations (Fig. 4A and Supplementary Table S2; ref. 30). Following the dosing period, tumor growth in the 1 mg/kg cohort rebounded rapidly (TGD = 21 days), whereas the 10 mg/kg cohort showed sustained tumor remission up to 30 days following the final dose of quizartinib (TGD = 55 days). Remarkably, after a single 10 mg/kg dose of quizartinib, no tumor growth was observed for up to 2 weeks (TGD = 15 days). Even a single 1 mg/kg dose of quizartinib caused significant reduction in tumor growth (TGD = 5 days; Fig. 4A and Supplementary Table S2).

To determine whether differences in tumor volume reduction between single doses of 1 versus 10 mg/kg quizartinib correlated with pharmacodynamic assessments, levels of pFLT3, pErk1/2, pSTAT5, and pAkt at various times following drug administration were assessed in tumor lysates. Quizartinib administration leads to a rapid decrease in FLT3, STAT5, and Erk1/2 phosphorylation in the tumors at both doses tested (Fig. 4B). The 1 mg/kg dose reduced FLT3 phosphorylation by 60% at 2 hours, reached maximal inhibition of approximately 70% by 6 hours and had recovered to within 20% of control levels by 24 hours. STAT5 phosphorylation followed a similar pattern following the 1 mg/kg dose with 40% inhibition at 2 hours, 75% inhibition at 6 hours, and full recovery at 24 hours. Inhibition of Erk1/2 phosphorylation was not as robust with inhibition levels of 30% at both 2 and 6 hours and control levels returning by 24 hours. Akt phosphorylation was not impacted following a 1 mg/kg dose of quizartinib. At 10 mg/kg, the impact on signaling was much more pronounced with 80% inhibition of pFLT3 observed at both the 2- and 6-hour time points and a residual 50% inhibition at 24 hours. Similarly, pErk1/2 levels were reduced by roughly 70% at 2 and 6 hours, returning to within 30% inhibition by 24 hours. More striking was the effect of 10 mg/kg on STAT5 phosphorylation, which was reduced by more than 95% at all 3 time points. Consistent with the effect at the 1 mg/kg dose, the 10 mg/kg dose only modestly inhibited (10%–15%) Akt phosphorylation at 2 and 6 hours with pAkt levels elevated at 24 hours.

Finally, to determine whether the rapid loss of tumor volume was associated with an induction of apoptosis, cleavage of PARP was followed in tumor lysates. Tumors from mice receiving either 1 or 10 mg/kg showed considerable PARP cleavage 2 and 6 hours posttreatment with the peak of cleavage occurring at the 6-hour time point (Fig. 4C). In the 1 mg/kg tumor lysates, no additional PARP cleavage was observed at 24 hours, whereas in the 10 mg/kg lysates, PARP cleavage remained elevated. These experiments suggest that the degree of sustained antitumor activity achieved appears to correlate with the durability of FLT3 signal inhibition within the first 24 hours and may reflect durable inhibition of FLT3 in residual tumor cells.

Discussion

Although clinical activity has been observed with first-generation FLT3 inhibitors, as a class they have failed to fulfill the promise of providing long-term therapeutic benefit in AMLs (15–17, 21, 22, 29). Potential explanations for these marginal clinical results include insufficient FLT3 potency leading to residual disease and/or inadequate FLT3 selectivity leading to off-target effects and associated dose-limiting toxicity (2, 14, 22). Among responders to these first-generation FLT3 inhibitors, patients with FLT3-ITD mutations were in the clear

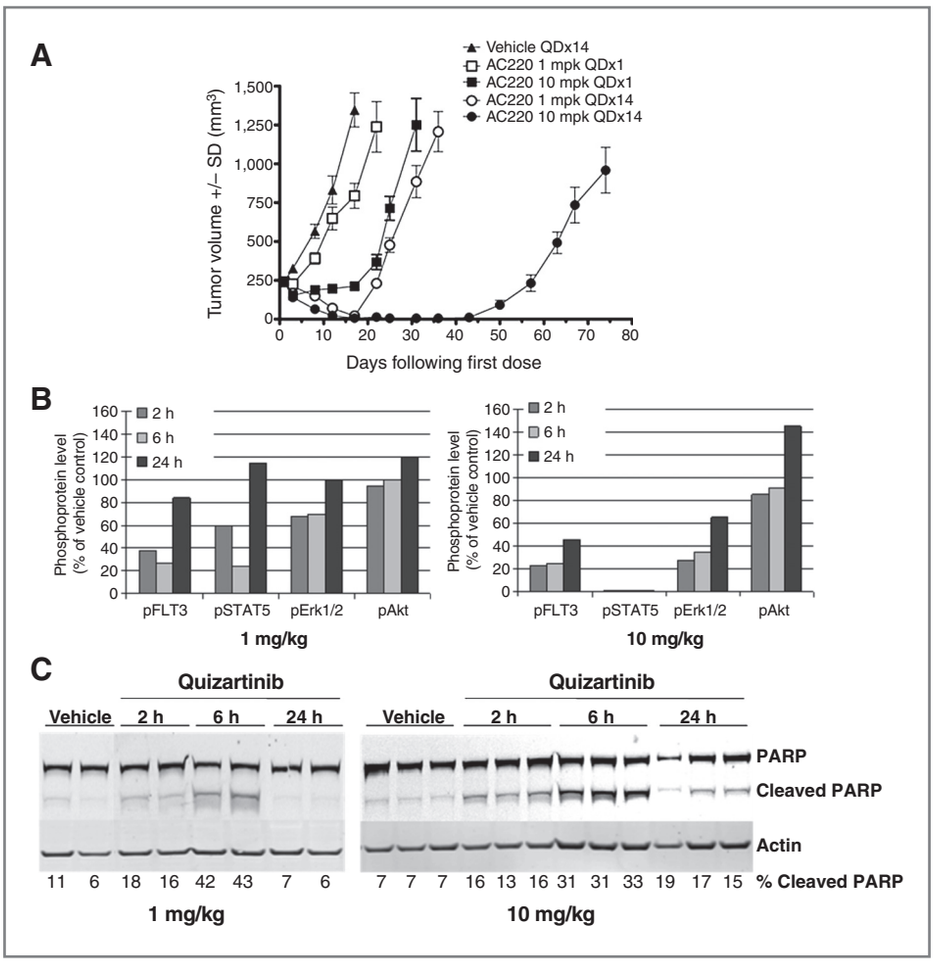

Figure 4. Durability of efficacy with a single dose of quizartinib in MV4-11 xenograft tumors. A, mice bearing MV4-11 xenograft tumors were treated with drug vehicle or 1 or 10 mg/kg of quizartinib orally once daily (QD) for 1 or 14 days. B, time course of FLT3, STAT5, Erk1/2, or Akt phosphorylation levels in MV4-11 tumor lysates from ($n = 3$) animals treated with a single oral dose of 1 or 10 mg/kg of quizartinib. C, immunoblot analysis of PARP cleavage in tumor treated with vehicle or a single dose of 1 or 10 mg/kg quizartinib.

majority; however, a smaller number of ITD-negative patients also responded to therapy (38, 39). In the preclinical studies presented here, we characterize quizartinib with respect to potency and durability of inhibition against WT and ITD-mutant FLT3 kinase across a panel of cells harboring distinct *FLT3* genotypes, compare these properties to a panel of first- and second-generation FLT3 inhibitors, and show that quizartinib possesses slow off-rate kinetics. These studies showed that (i) quizartinib potently inhibits cellular signaling in both ITD and WT cells, yet translation to induction of apoptosis was restricted to cells with constitutive FLT3 activation, whether ITD or WT; (ii) as a result of slow off-rate kinetics, quizartinib requires only transient exposures to effect durable inhibition of FLT3, its downstream signaling pathways, and ultimately cell viability in FLT3-dependent cells *in vitro*

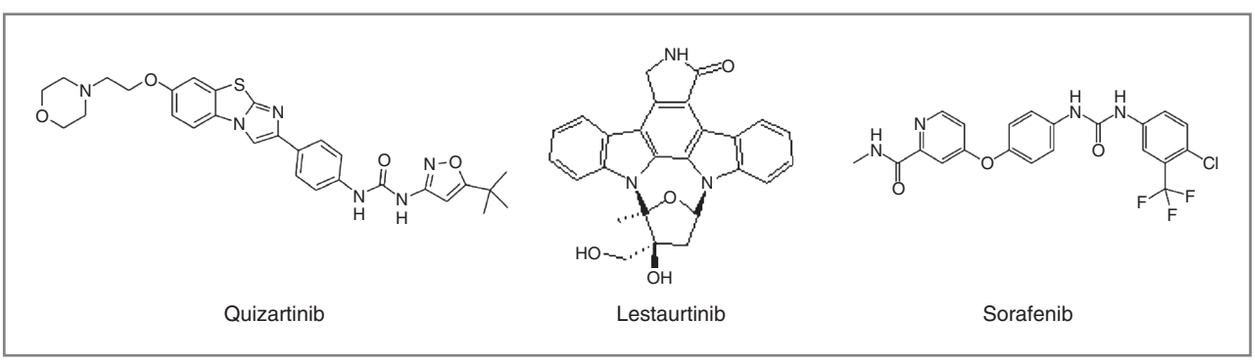

Figure 5. Chemical structures of FLT3 inhibitors.

and *in vivo*; and finally, (iii) quizartinib is unique among current FLT3 inhibitors in this profile of selectivity across the kinome, potency against cellular FLT3, and durability of inhibition once achieved.

The ability of quizartinib to distinguish FLT3-dependent from FLT3-independent cells may be important for 2 reasons. First, this profile suggests that quizartinib therapy may spare cells not directly reliant upon FLT3 activity for survival. As not all FLT3 inhibitors are able to make this distinction (Supplementary Table S1 and ref. 30), tolerability issues associated with these inhibitors may be attributed to off-target–mediated induction of apoptosis in non–FLT3-dependent cells. Second, quizartinib-induced apoptosis in FLT3-WT–activated cells (SEM-K2) is reminiscent of the clinical experience where a significant minority of responding patients lacked the FLT3 ITD. Defining the molecular mechanisms responsible for this FLT3 dependency in the ITD-negative population is the subject of current preclinical and clinical investigation.

A common challenge in the clinical development of kinase inhibitors has been the inability to maintain prolonged target inhibition without exceeding tolerated levels of the drug. While TKIs including lestaurtinib and midostaurin have shown transient clinical responses, other inhibitors such as sorafenib and dasatinib have shown more durable responses with target inhibition sustained after efficacious levels of drug have been eliminated *in vivo* or washed away *in vitro* (17, 22, 40–42). In the studies reported here, reduction of FLT3 phosphorylation and downstream signaling is maintained for up to 24 hours after quizartinib is removed from culture, and an exposure time as low as 30 minutes was as effective as a 72-hour incubation to induce cell death in sensitive cells. *In vivo*, this durability contributes to sustained inhibition of FLT3, STAT5, and ERK phosphorylation after a single dose, and long after the majority of the administered quizartinib has been eliminated from peripheral circulation. Our binding studies suggest that slow dissociation of quizartinib from FLT3 may contribute to enhanced efficacy relative to a simple pharmacokinetic "time-over-target" estimation. Similar to our findings with quizartinib, slow inhibitor off-rates have been shown to mediate durable target inhibition for other kinase inhibitors (43).

Quizartinib appears to be unique among the panel of tested inhibitors on several accounts. Although lestaurtinib and sorafenib showed similar potency to quizartinib with respect to FLT3 inhibition, lestaurtinib and to a lesser degree sorafenib retained significant activity against the non–FLT3-activated cells (ref. 30 and Supplementary Table S1). This theme was repeated with respect to durability of inhibition in that quizartinib showed significantly enhanced durability of efficacy and slower binding kinetics relative to lestaurtinib. In a recent report comparing quizartinib with lestaurtinib in blasts derived from a small cohort of patients with AMLs, the authors suggest that a less selective FLT3 inhibitor such as lestaurtinib may be more effective at first diagnosis than a more selective inhibitor such as quizartinib (44). While confirmation of this hypothesis awaits a side-by-side comparison of clinical results, it is quite plausible that the degree to which blasts are addicted to FLT3 signaling (and therefore respond to a FLT3-selective inhibitor) may vary in the heterogeneous AML patient population, especially at first diagnosis. Regardless of the potential for a more modest initial response compared with the multi-kinase inhibitors, the prolonged efficacy after a brief exposure *in vivo*, along with its potency, durability, and selectivity *in vitro*, may bode well for the safe, durable, and efficacious use of quizartinib in the clinic.

Disclosure of Potential Conflicts of Interest

No potential conflicts of interest were disclosed.

Authors' Contributions

Conception and design: R.N. Gunawardane, B. Belli, R.C. Armstrong
Development of methodology: R.N. Gunawardane, R.R. Nepomuceno, J. P. Hunt, B. Belli, R.C. Armstrong
Acquisition of data (provided animals, acquired and managed patients, provided facilities, etc.): R.N. Gunawardane, R.R. Nepomuceno, A.M. Rooks, J.P. Hunt, J.M. Ricono
Analysis and interpretation of data (e.g., statistical analysis, biostatistics, computational analysis): R.N. Gunawardane, R.R. Nepomuceno, J.P. Hunt, J.M. Ricono, B. Belli, R.C. Armstrong
Writing, review, and/or revision of the manuscript: R.N. Gunawardane, R.R. Nepomuceno, J.P. Hunt, J.M. Ricono, R.C. Armstrong
Administrative, technical, or material support (i.e., reporting or organizing data, constructing databases): R.N. Gunawardane, R.C. Armstrong
Study supervision: R.N. Gunawardane, B. Belli, R.C. Armstrong

Acknowledgments

The authors thank M. Holladay, P. Zarrinkar, and W. Wierenga for thoughtful discussions and critical reading of the manuscript and R Faraoni, M. Hocker, and B. Campbell for synthesis of midostaurin, lestaurtinib, sorafenib, and quizartinib.

The costs of publication of this article were defrayed in part by the payment of page charges. This article must therefore be hereby marked *advertisement* in accordance with 18 U.S.C. Section 1734 solely to indicate this fact.

Received March 30, 2012; revised January 8, 2013; accepted January 29, 2013; published OnlineFirst February 14, 2013.

References

1. Stirewalt DL, Radich JP. The role of FLT3 in haematopoietic malignancies. Nat Rev Cancer 2003;3:650–65.
2. Kindler T, Lipka DB, Fischer T. FLT3 as a therapeutic target in AML: still challenging after all these years. Blood 2010;116:5089–102.
3. Kiyoi H, Towatari M, Yokota S, Hamaguchi M, Ohno R, Saito H, et al. Internal tandem duplication of the FLT3 gene is a novel modality of elongation mutation which causes constitutive activation of the product. Leukemia 1998;12:1333–7.
4. Abu-Duhier FM, Goodeve AC, Wilson GA, Gari MA, Peake IR, Rees DC, et al. FLT3 internal tandem duplication mutations in adult acute myeloid leukaemia define a high-risk group. Br J Haematol 2000; 111:190–5.

5. Cloos J, Goemans BF, Hess CJ, van Oostveen JW, Waisfisz Q, Corthals S, et al. Stability and prognostic influence of FLT3 mutations in paired initial and relapsed AML samples. Leukemia 2006; 20:1217–20.
6. Gilliland DG, Griffin JD. The roles of FLT3 in hematopoiesis and leukemia. Blood 2002;100:1532–42.
7. Whitman SP, Archer KJ, Feng L, Baldus C, Becknell B, Carlson BD, et al. Absence of the wild-type allele predicts poor prognosis in adult de novo acute myeloid leukemia with normal cytogenetics and the internal tandem duplication of FLT3: a cancer and leukemia group B study. Cancer Res 2001;61:7233–9.
8. Ozeki K, Kiyoi H, Hirose Y, Iwai M, Ninomiya M, Kodera Y, et al. Biologic and clinical significance of the FLT3 transcript level in acute myeloid leukemia. Blood 2004;103:1901–8.
9. Brandts CH, Sargin B, Rode M, Biermann C, Lindtner B, Schwable J, et al. Constitutive activation of Akt by Flt3 internal tandem duplications is necessary for increased survival, proliferation, and myeloid transformation. Cancer Res 2005;65:9643–50.
10. Choudhary C, Brandts C, Schwable J, Tickenbrock L, Sargin B, Ueker A, et al. Activation mechanisms of STAT5 by oncogenic Flt3-ITD. Blood 2007;110:370–4.
11. Hayakawa F, Towatari M, Kiyoi H, Tanimoto M, Kitamura T, Saito H, et al. Tandem-duplicated Flt3 constitutively activates STAT5 and MAP kinase and introduces autonomous cell growth in IL-3-dependent cell lines. Oncogene 2000;19:624–31.
12. Mizuki M, Fenski R, Halfter H, Matsumura I, Schmidt R, Muller C, et al. Flt3 mutations from patients with acute myeloid leukemia induce transformation of 32D cells mediated by the Ras and STAT5 pathways. Blood 2000;96:3907–14.
13. Rocnik JL, Okabe R, Yu JC, Lee BH, Giese N, Schenkein DP, et al. Roles of tyrosine 589 and 591 in STAT5 activation and transformation mediated by FLT3-ITD. Blood 2006;108:1339–45.
14. Levis M, Small D. FLT3 tyrosine kinase inhibitors. Int J Hematol 2005;82:100–7.
15. DeAngelo DJ, Stone RM, Heaney ML, Nimer SD, Paquette RL, Klisovic RB, et al. Phase 1 clinical results with tandutinib (MLN518), a novel FLT3 antagonist, in patients with acute myelogenous leukemia or high-risk myelodysplastic syndrome: safety, pharmacokinetics, and pharmacodynamics. Blood 2006;108:3674–81.
16. Fiedler W, Serve H, Dohner H, Schwittay M, Ottmann OG, O'Farrell AM, et al. A phase 1 study of SU11248 in the treatment of patients with refractory or resistant acute myeloid leukemia (AML) or not amenable to conventional therapy for the disease. Blood 2005;105:986–93.
17. Knapper S, Burnett AK, Littlewood T, Kell WJ, Agrawal S, Chopra R, et al. A phase 2 trial of the FLT3 inhibitor lestaurtinib (CEP701) as first-line treatment for older patients with acute myeloid leukemia not considered fit for intensive chemotherapy. Blood 2006;108:3262–70.
18. O'Farrell AM, Abrams TJ, Yuen HA, Ngai TJ, Louie SG, Yee KW, et al. SU11248 is a novel FLT3 tyrosine kinase inhibitor with potent activity *in vitro* and *in vivo*. Blood 2003;101:3597–605.
19. O'Farrell AM, Foran JM, Fiedler W, Serve H, Paquette RL, Cooper MA, et al. An innovative phase I clinical study demonstrates inhibition of FLT3 phosphorylation by SU11248 in acute myeloid leukemia patients. Clin Cancer Res 2003;9:5465–76.
20. Smith BD, Levis M, Beran M, Giles F, Kantarjian H, Berg K, et al. Single-agent CEP-701, a novel FLT3 inhibitor, shows biologic and clinical activity in patients with relapsed or refractory acute myeloid leukemia. Blood 2004;103:3669–76.
21. Stone RM, DeAngelo DJ, Klimek V, Galinsky I, Estey E, Nimer SD, et al. Patients with acute myeloid leukemia and an activating mutation in FLT3 respond to a small-molecule FLT3 tyrosine kinase inhibitor, PKC412. Blood 2005;105:54–60.
22. Wiernik PH. FLT3 inhibitors for the treatment of acute myeloid leukemia. Clin Adv Hematol Oncol 2010;8:429–44.
23. Auclair D, Miller D, Yatsula V, Pickett W, Carter C, Chang Y, et al. Antitumor activity of sorafenib in FLT3-driven leukemic cells. Leukemia 2007;21:439–45.
24. Kelly LM, Yu JC, Boulton CL, Apatira M, Li J, Sullivan CM, et al. CT53518, a novel selective FLT3 antagonist for the treatment of acute myelogenous leukemia (AML). Cancer Cell 2002;1:421–32.
25. Levis M, Allebach J, Tse KF, Zheng R, Baldwin BR, Smith BD, et al. A FLT3-targeted tyrosine kinase inhibitor is cytotoxic to leukemia cells *in vitro* and *in vivo*. Blood 2002;99:3885–91.
26. Pratz KW, Cortes J, Roboz GJ, Rao N, Arowojolu O, Stine A, et al. A pharmacodynamic study of the FLT3 inhibitor KW-2449 yields insight into the basis for clinical response. Blood 2009;113:3938–46.
27. Shankar DB, Li J, Tapang P, Owen McCall J, Pease LJ, Dai Y, et al. ABT-869, a multitargeted receptor tyrosine kinase inhibitor: inhibition of FLT3 phosphorylation and signaling in acute myeloid leukemia. Blood 2007;109:3400–8.
28. Weisberg E, Boulton C, Kelly LM, Manley P, Fabbro D, Meyer T, et al. Inhibition of mutant FLT3 receptors in leukemia cells by the small molecule tyrosine kinase inhibitor PKC412. Cancer Cell 2002;1: 433–43.
29. Pratz KW, Levis MJ. Bench to bedside targeting of FLT3 in acute leukemia. Curr Drug Targets 2010;11:781–9.
30. Zarrinkar PP, Gunawardane RN, Cramer MD, Gardner MF, Brigham D, Belli B, et al. AC220 is a uniquely potent and selective inhibitor of FLT3 for the treatment of acute myeloid leukemia (AML). Blood 2009;114: 2984–92.
31. Levis M, Brown P, Smith BD, Stine A, Pham R, Stone R, et al. Plasma inhibitory activity (PIA): a pharmacodynamic assay reveals insights into the basis for cytotoxic response to FLT3 inhibitors. Blood 2006;108: 3477–83.
32. Zhang W, Konopleva M, Shi YX, McQueen T, Harris D, Ling X, et al. Mutant FLT3: a direct target of sorafenib in acute myelogenous leukemia. J Natl Cancer Inst 2008;100:184–98.
33. Wodicka LM, Ciceri P, Davis MI, Hunt JP, Floyd M, Salerno S, et al. Activation state-dependent binding of small molecule kinase inhibitors: structural insights from biochemistry. Chem Biol 2010;17: 1241–9.
34. Bissery MC, Guenard D, Gueritte-Voegelein F, Lavelle F. Experimental antitumor activity of taxotere (RP 56976, NSC 628503), a taxol analogue. Cancer Res 1991;51:4845–52.
35. Quentmeier H, Reinhardt J, Zaborski M, Drexler HG. FLT3 mutations in acute myeloid leukemia cell lines. Leukemia 2003;17:120–4.
36. Spiekermann K, Bagrintseva K, Schwab R, Schmieja K, Hiddemann W. Overexpression and constitutive activation of FLT3 induces STAT5 activation in primary acute myeloid leukemia blast cells. Clin Cancer Res 2003;9:2140–50.
37. Lierman E, Lahortiga I, Van Miegroet H, Mentens N, Marynen P, Cools J. The ability of sorafenib to inhibit oncogenic PDGFRbeta and FLT3 mutants and overcome resistance to other small molecule inhibitors. Haematologica 2007;92:27–34.
38. Brown P, Meshinchi S, Levis M, Alonzo TA, Gerbing R, Lange B, et al. Pediatric AML primary samples with FLT3/ITD mutations are preferentially killed by FLT3 inhibition. Blood 2004;104:1841–9.
39. Levis M, Tse KF, Smith BD, Garrett E, Small D. A FLT3 tyrosine kinase inhibitor is selectively cytotoxic to acute myeloid leukemia blasts harboring FLT3 internal tandem duplication mutations. Blood 2001;98:885–7.
40. Pratz KW, Cho E, Karp JE, Levis M, Zhao M, Rudek M, et al. Phase I dose escalation trial of sorafenib as a single agent for adults with relapsed and refractory acute leukemias. J Clin Oncol 2009;27:abstr 7065.
41. Safaian NN, Czibere A, Bruns I, Fenk R, Reinecke P, Dienst A, et al. Sorafenib (Nexavar) induces molecular remission and regression of extramedullary disease in a patient with FLT3-ITD+ acute myeloid leukemia. Leuk Res 2009;33:348–50.
42. Snead JL, O'Hare T, Adrian LT, Eide CA, Lange T, Druker BJ, et al. Acute dasatinib exposure commits Bcr-Abl-dependent cells to apoptosis. Blood 2009;114:3459–63.
43. Wood ER, Truesdale AT, McDonald AB, Derek Y, Hassell A, Dickerson SH, et al. A unique structure for epidermal growth factor receptor bound to GW572016(Lapatinib): relationships among protein conformation, inhibitor off-rate, and receptor activity in tumor cells. Cancer Res 2004;64:6652–9
44. Pratz KW, Sato T, Murphy KM, Stine A, Rajkhowa T, Levis M. FLT3-mutant allelic burden and clinical status are predictive of response to FLT3 inhibitors in AML. Blood 2010;115:1425–32.